



## Scour prevention in bottomless arch culverts

B. M. CROOKSTON<sup>1</sup> and B. P. TULLIS<sup>2</sup>

### Abstract

Bottomless arch culverts are employed as ecological bridges at road crossings with their most common application being fish passage. The simulated culvert streambed should mimic the existing natural channel but be engineered to resist erosion during high flow events. To provide some design guidance for simulated streambed stability in culverts, a culvert streambed stability study was conducted using a 0.61-m (2-ft) diameter smooth-walled bottomless arch culvert featuring streambed materials ranging in size from pea gravel to cobbles. Several culvert entrance geometries over a range of headwater depths (unsubmerged and submerged inlet conditions) were evaluated. Eight riprap stone-sizing stability relationships were evaluated, relative to the experimental data, to determine their potential applicability to arched bottomless culverts streambed stability design. Some general observations are discussed regarding the location and extent of scour events in bottomless culverts and incipient motion velocity variations between the bottomless arched culvert and a rectangular flume for the same substrate materials.

**Key Words:** Scour prevention, Bottomless arch culvert, Fish passage, Riprap, Gravel streambed

### 1 Introduction

Due to the increasing demand for habitat protection and ecological connectivity at road crossings, alternatives to traditional culvert designs are being implemented. One alternative is a bottomless arch culvert with a simulated streambed representing the culvert invert. Such culverts are designed to not only mimic the natural streambed, but also to facilitate natural stream processes such as sediment transport, flood routing, and debris conveyance. Such designs can also address the requisite hydraulic conditions of specific aquatic species that must navigate the culvert.

Design criteria for fish passage bottomless arch culverts have been developed or adopted by various state and federal agencies, such as the State of California Department of Fish and Game (2002) and the Washington Department of Fish and Wildlife (Bates et al., 2003). Some general design guidelines include matching the culvert entrance and exit elevations and slope with the adjacent stream channel. Culvert skew should be minimized to prevent head-cutting and the bottomless arch culvert width should be equal to or greater than the bank-full channel width. In addition, the simulated channel should provide ecologically acceptable hydraulic conditions under base flows, such as navigable velocities for fish. The streambed inside the culvert should simulate the native streambed, however, the streambed substrate material should also be sized to minimize scour at high flow rates to maintain structural integrity.

Scour associated with traditional circular culverts has been of interest for decades. Investigations regarding impinging jets (Abt et al., 1984); cohesive (Abt, 1980) and cohesionless streambed materials (Chien et al., 1998); tailwater, discharge, and culvert cross-section influences (Bohan, 1970; Abida and

---

<sup>1</sup> Postdoctoral Researcher, Utah Water Research Laboratory, Utah State University, 8200 Old Main Hill, Logan, UT 84322, E-mail: [bcrookston@gmail.com](mailto:bcrookston@gmail.com), [bcrookston@schnebel-eng.com](mailto:bcrookston@schnebel-eng.com)

<sup>2</sup> Assoc. Prof., Utah State University, Utah Water Research Laboratory, 8200 Old Main Hill, Logan, UT 84322, E-mail: [blake.tullis@usu.edu](mailto:blake.tullis@usu.edu)

Note: The original manuscript of this paper was received in Mar. 2011. The revised version was received in Apr. 2012. Discussion open until Mar. 2013.

Townsend, 1991); culvert slope (Abt et al., 1985); and headwall and wingwall effects (Mendoza et al., 1983) have been undertaken in an effort to predict and control the amount of scour occurring at non-embedded culvert inlets, outlets, and adjacent regions (Abt and Thompson, 1996). Riprap protection (HEC-14, 1983) and incipient motion relationships for impinging jets (Shafai-Bajestan and Albertson, 1993) at culvert outlets have been developed to protect against perched outlets and possible failure of the structure. Very little work, however, has been done specific to scour in bottomless culverts.

In an effort to provide much needed information regarding the performance of existing riprap design methods for bottomless arch culverts, eight predictive methods were selected and compared with a bottomless arch culvert scour data collected in the laboratory. Methods 1–8 are presented in Table 1 along with the application specific to that method.

**Table 1** Riprap stone size design equations

Design method	Equation	Reference	Development application	Comments
1	$d_{50} = \frac{0.69V_{eff}^2}{2g(SG-1)}$	FHWA-RD-02-078 (2003)	Bottomless Arch Culverts ( $D = 0.61$ m)	Based upon Ishbash method and effective velocity prediction method $V_{eff}$ = effective local velocity at culvert entrance
2	$d_{50} = \frac{0.38Y_{ent}}{SG-1} \left( \frac{V_{ent}^2}{gY_{ent}} \right)^{0.33}$	FHWA-HRT-07-026 (2007)	Bottomless Box Culvert (0.61-m wide and 0.15-m high)	Based upon experimental results $V_{ent}$ = average entrance velocity
3	$d_{50} = 0.01V^{2.44}$	Halvorson and Laumann (1996)	Concrete arch on spread footings, 100 year flood event	Based upon field data
4	$d_{50} = \frac{CV^{3.95}}{Y^{1.06}}$	FHWA HEC-11 (1989)	Upstream slope of earth dams	Limited to subcritical flow, angular material $C=0.00117$
5	$d_{50} = \left( \frac{0.0000212836 V^6 SG}{(SG-1)^3} * \frac{6}{\pi\gamma_s} \right)^{\frac{1}{3}}$	California Department of Public Works, Division of Highways (1970)	Riprap for banks and shores	Based upon wave theory and force-energy relationships. Experimental results
6	$d_{30} = C_V C_T Y \frac{d_{84}}{d_{16}} \left[ \left( \frac{\gamma}{\gamma_s - \gamma} \right)^{\frac{1}{2}} \frac{V}{\sqrt{gY}} \right]^{-2.5}$	EM-1110-2-1601 (1994)	Channel banks	$C_V = 1$ $C_T = d_{100}$ or $1.5d_{50}$
7	$d_{50} = \left( \frac{0.000041 SG V^6}{(SG-1)^3} * \frac{6}{\pi\gamma_s} \right)^{\frac{1}{3}}$	ASCE Manual 54 (Vanoni, 2004)	Riprap protection of banks	Graded materials used on Missouri River
8	$d_{40} = 0.0105(V)^{2.6}$	USBR-EM-25 (1965)	Channels downstream of stilling Basins	Laboratory experimental results, uses velocity on channel bottom

The Federal Highway Administration (FHWA) conducted a two-phase study exploring bottomless culvert inlet and/or outlet scour. Phase 1 (FHWA-RD-02-078) tested 0.6-m wide scale models of four commercially available, bottomless culvert shapes using different uniformly graded sand substrate

materials. Phase 2 (FHWA-HRT-07-026) explored riprap sizing requirements at the inlet and outlet of a rectangular bottomless culvert (0.61-m wide and 0.15-m high) with vertical wing walls using uniformly graded gravel. The results of Phases 1 and 2 are methods 1 and 2, respectively.

To develop method 3, Halvorson and Laumann (1996) evaluated several traditional riprap design methods [FHWA HEC-11 (1989), Blodgett and McConaughy (1986), and Maynard (1979; 1987)], using field data from a concrete arch on spread footings. Method 4 comes from HEC-11 (FHWA HEC-11, 1989), which is based upon tractive force theory and is limited to subcritical flow, angular bed materials, and utilizes velocity and flow depth as design parameters. The California Department of Public Works, Division of Highways (1970) published method 5, which was developed based on wave induced bank scour.

The U.S. Army Corp of Engineers (USACE, 1994) developed method 6, which includes several user-defined coefficients, (described in Table 1) which have a significant impact on the method's accuracy and should be based on site-specific field observations.

Method 7 comes from the ASCE Manual 54 (Vanoni, 2004). Method 8 was developed by the United States Bureau of Reclamation (USBR-EM-25, 1965) by Blodgett and McConaughy specifically to scour protection downstream of stilling basins. The published equations for methods 5 and 7 have been modified in the current study to predict a spherical stone diameter instead of stone weight.

Methods 5–8 are well established methods used in riprap protection of open channels; Methods 1 and 2 were specifically developed for bottomless culverts, though limited to the culvert inlet and outlet. Method 3 is specific to concrete arches, which is similar to a bottomless arch culvert, but focused on a specific flood event (100-yr). No previous studies have provided information regarding the extent to which scour occurs within a bottomless arch culvert or the performance of riprap stone sizing methods.

The objectives of this study were to observe the response of various substrate materials inside a 0.61-m (2-ft) diameter bottomless arch culvert for various flow conditions (pressurized and non-pressurized culvert flow) and inlet geometries; observations included particle transport, bedforms, and scour depths. Incipient motion of the substrate materials and inlet geometries were evaluated inside the bottomless arch culvert and in a 0.30-m (1-ft) wide rectangular laboratory flume for comparison. Using the incipient motion velocity and other necessary system parameters, the required stable riprap size was estimated using each method in Table 1 and compared with the corresponding experimental substrate size parameter. The ratio of the predicted to actual stone size values ( $d_{s-pred}/d_{s-actual}$ ) for each method represents a stone-size prediction factor of safety ( $SF$ ).

## 2 Experimental method

### 2.1 Facility

All research was conducted at the Utah Water Research Laboratory (UWRL) at Utah State University (Crookston, 2008). The incipient motion characteristics of the test substrates were evaluated using two different facilities at the UWRL—a bottomless culvert facility and a rectangular flume (Crookston and Tullis, 2011).

The bottomless culvert test facility featured a head box (2.44-m (8-ft) wide by 1.07-m (3.5-ft) deep by 5.33-m (17.5-ft) long) and tail box (2.44-m (8-ft) wide by 1.07-m (3.5-ft) deep by 5.33-m (17.5-ft) long) connected by a 0.61-m diameter bottomless circular arch culvert as shown in Fig. 1. The 4.88-m (16-ft) long arched (half-cylinder) bottomless culvert, fabricated using clear acrylic for flow visualization, was installed on top of a 0.61-m wide by 0.33-m (13-in) deep (rectangular cross section) steel box filled with substrate material. The culvert assembly was set at a slope of 0.01. The 2.44-m wide approach channel (the width of the head box) and movable 90° wing walls facilitated a reasonable range of inlet flow contraction variation.

A rectangular flume with acrylic walls was also used in this study. The test section in the flume was 0.30-m (1-ft) wide, 0.61-m (2-ft) deep, and 5.2-m (17-ft) long and a 100-mm deep recess were filled with the tested substrate materials.

### 2.2 Substrate materials

Four substrate materials (referred to by their approximate  $d_m$  value) were tested, 7-mm (0.25-in) pea gravel, 16-mm (0.6-in) angular gravel, 35-mm (1.4-inch) rounded cobbles and 37-mm (1.5-inch) angular

rock. These materials were selected to represent armored, non-cohesive streambeds. Sieve and density analyses were conducted for each substrate material and the results are summarized in Table 2.

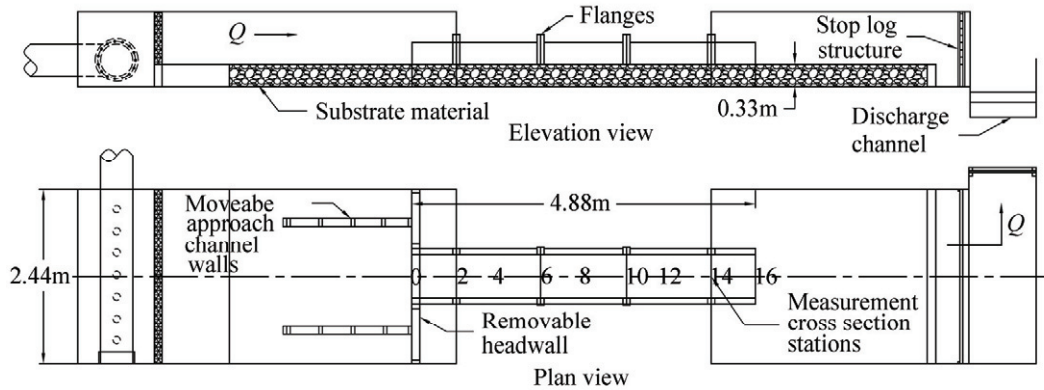


**Fig. 1** Overview of bottomless arch culvert test facility

**Table 2** Substrate sieve analyses results

Size	7-mm	16-mm	35-mm	37-mm
Fraction	Gravel	Angular Gravel	Cobbles	Angular Rock
$D_{16}$ (mm)	4.30	12.75	26.80	24.17
$D_{35}$ (mm)	5.80	14.70	30.50	31.81
$D_{50}$ (mm)	6.75	16.15	33.00	37.37
$D_{65}$ (mm)	7.80	17.40	36.00	42.78
$D_m$ (mm)	6.60	16.05	34.82	37.16
$D_{84}$ (mm)	9.40	20.50	43.50	49.72
$D_{95}$ (mm)	11.20	23.40	56.00	57.5
SG	2.48	2.46	2.58	2.42
$\gamma$ ( $N\ m^{-3}$ )	24,318	24,103	25,276	23,686

### 2.3 Testing procedure

In the bottomless culvert test facility, each substrate material was placed upstream, inside, and downstream of the culvert. The elevation of the top of the material was meticulously graded to correspond with the elevation of the top of the steel box/culvert interface (i.e., culvert spring-line). For each substrate material, five entrance configurations were tested featuring three different inlet contraction ratios (0%, 33% and 75%) for both projecting and non-projecting (headwall) entrance conditions. The 0% contraction configuration was limited to the non-projecting condition. Collected test data included incipient motion velocities, depths of scour, and extent of scour. Examples of three entrance configurations (two pre- and one post-test condition) are presented in Fig. 2.



**Fig. 2** Examples of bottomless arch culvert entrance conditions (A=0%, B=33%, C=75% approach channel to culvert inlet contraction ratios)

Each substrate and inlet configuration was tested over a range of headwater depths. Headwater depths were expressed dimensionless as the headwater depth measured relative to the pre-scour invert at the culvert entrance over the pre-scour culvert height,  $H_w/D$  (Fig. 3). The headwater depth was measured in a corner of the headbox adjacent to the culvert entrance, where the velocity was negligible and the headwater depth,  $H_w$ , represented the total energy head at the culvert entrance. A summary of the  $H_w/D$  ratios tested for each substrate material is presented in Table 3.

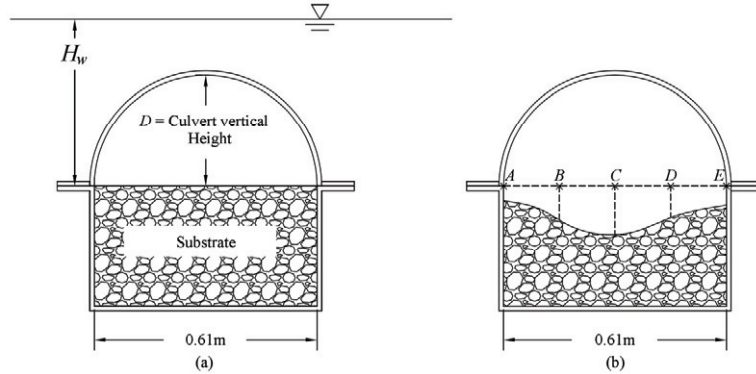


Fig. 3 Schematics of (A)  $H_w/D$  and (B) culvert cross-section scour depth measurement locations

Table 3  $H_w/D$  test ratios

		16-mm		37-mm
	7-mm	Angular	35-mm	Angular
$H_w/D$	Gravel	Gravel	Cobbles	Rock
0.5	x			
1.0		x	x	x
1.5			x	x

There was no controlled tailwater at the exit of the culvert, no end sill to influence scour, and all tests consisted of a 0.61-m projecting end treatment with a 400% expansion from the culvert into the tailbox. Thirty-five separate tests were conducted from the combination of contraction ratios, tested headwater depths, and streambed materials.

Testing in the rectangular flume focused on incipient motion of the substrate particles. A 100-mm deep layer of substrate material was tested at three different bed slopes (0.005, 0.01, and 0.015); the 0.01 slope tested corresponded to the tested culvert slope. Twelve separate tests were performed and each test was duplicated to monitor repeatability and results sensitivity. Flow rates through the culvert test facility and the laboratory flume were metered using calibrated orifice plate flow meters in the supply piping. Water entered the culvert test facility head box through a diffuser and passed through a baffle wall, which created a relatively uniform approach flow upstream of the culvert. The flume also featured a diffuser on the supply end.

#### 2.4 Data collection

The scour test duration for a specific  $H_w/D$  condition was approximately 2 hours, which is referred to as a duration test. This test duration was based upon preliminary test investigations for this study, which observed scour rates for up to 24 hours, time requirements for scour equilibrium, and any formation and migration of bedforms. Data collection included flow rate, water surface profiles, streambed profiles, and location specific bed velocities.

Each test began by slowly increasing the flow rate into the system, to prevent any premature scouring, and permitted monitoring of the bed for incipient motion. Incipient motion is statistical by nature and is difficult to determine in turbulent flows. Visual observation was selected to detect incipient motion for the ability to witness the response of individual grains to flow conditions and location in the culvert. This method is subjective and no standardized definition for the threshold of movement for mixed sediment was located in literature. In this study, the authors defined incipient motion as the flow condition

producing approximately 10 moving particles per minute at a specific location (Crookston and Tullis, 2011). This standard is within the limit ( $\varepsilon=1\text{E-}6$ ) proposed by Yalin (1972), defined by Eq. (1).

$$\varepsilon = \frac{N}{At} * \sqrt{\frac{\rho d_{50}^5}{(\gamma_s - \gamma)}} \quad (1)$$

In Eq. (1),  $\varepsilon$  is the criterion of incipient motion of a single grain size,  $N$  is the number of particles in motion in an observed area  $A$  for the time interval  $t$ ,  $\rho$  is the mass density of water,  $\gamma_s$  is the specific weight of sediment material, and  $\gamma$  is the specific weight of water. 10 particles per minute is equivalent to  $1.8\text{E-}6 \leq \varepsilon \leq 1.6 \text{E-}5$  for the bottomless culvert and  $1\text{E-}6 \leq \varepsilon \leq 3.2\text{E-}5$  for the flume. When incipient motion was reached, the flow rate was held constant and measurements were taken (flow rate, water surface profiles, bed velocities). Incremental flow rate increases were then resumed until the desired duration test  $H_w/D$  ratio was reached. The flow rate was held constant and measurements were taken in conjunction with any visual observations at 30-minute intervals during a two-hour period.

Bed velocity were measured using a propeller velocity probe with an accuracy of  $\pm 0.0015 \text{ m s}^{-1}$  ( $\pm 0.005 \text{ ft s}^{-1}$ ) at five locations (A, B, C, D, E, see Fig. 3) across the cross section at stations 0 and 16 (Fig. 1). During testing, the distance between the bed material and the bottom of the velocity probe was always minimized (approximately 5-mm). Water surface and bed profiles were measured in the headbox, tailbox, and at stations 0, 4, 8, 12, and 16 using a staff gauge readable to  $\pm 1.5\text{-mm}$  ( $\pm 0.06\text{-in}$ ). The station numbers represent the distance in feet between the culvert inlet and the measurement cross-section.

Following the duration test, the system was slowly drained of water and final scour measurements were made inside the culvert at stations 0, 1, 2, 4, 6, 8, 10, 12, 14, and 16; at five locations (A, B, C, D, E) across the cross-section of the culvert (Fig. 3). Geometries (shape, widths, and depths) were also taken at other locations where scour occurred, such as the scour at the culvert inlet and outlet.

The experimental methods used in the bottomless arch culvert were also applied to data collection in the rectangular flume facility. Velocities were measured with the propeller velocity probe at three stations along the length of the streambed.

### 3 Bottomless culvert scour results

#### 3.1 General scour observations

Yang and Simões (2005) suggested that suspended or washload materials, e.g., (dissolved material, clay, silt, and fine sand) can influence scour, however, the effects of washload were assumed negligible for this study and were not a controlled parameter. Washload was observable during testing of the 16-mm angular gravel and the 35-mm cobbles, which occurred during spring runoff when the water, supplied by the Logan River, was an opaque brown with limited visibility ( $<0.6\text{-m}$ ). The 7-mm gravel and the 37-mm angular rock were tested under clear water conditions.

The following discussion summarizes the general scour and deposition observations of the tested substrate materials inside the bottomless arch culvert. Substrate particles for all tested materials were observed to slide and roll along the bed. At higher flow rates, however, the 7-mm and 16-mm material saltated. Brief moments of particle suspension in the flow for the 7-mm gravel were observed; suspension was not limited to the culvert entrance where flow contraction and vortices were present. For all tested materials, scour was most severe at the entrance and the downstream half of the culvert, however, bed response was also observed to occur along the entire length of the culvert for certain test scenarios. Conical scour holes were observed at the edges of the culvert entrance, as shown in Fig. 4. Material removed from the entrance was generally deposited between stations 1 and 6 and at cross-section locations B, C, and D (Figs. 1 and 3). Particle transport inside the arch culvert for the tested materials often resulted in the deepest local scour depths near the middle of the cross section and the maximum overall depth of scour at or near the culvert outlet. As the flow exited the culvert, an oval scour hole was formed, as expected. The rate of scour decreased during the duration tests, eventually arriving at an approximate equilibrium condition. Finally, test scenarios that included a pressurized inlet resulted in an unstable or oscillating location where the water surface detached from the culvert crown. The detachment location would oscillate between station 4 and 14, often spending 2 to 5 minutes at a particular location before shifting again.

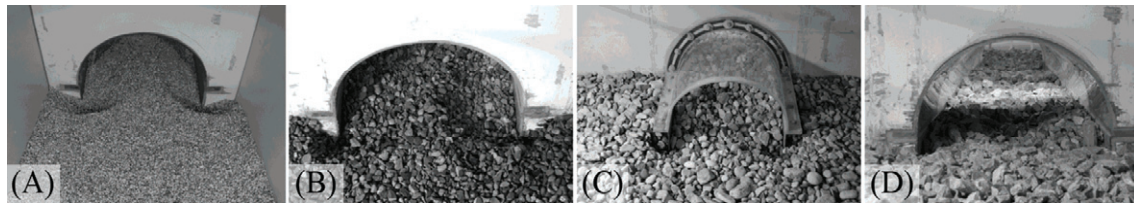


**Fig. 4** Examples of scour at entrance of culvert for (A) 7-mm gravel, (B) 16-mm angular gravel, (C) 35-mm cobbles, and (D) 37-mm angular rock

### 3.2 Extent of scour

For the 7-mm gravel substrate, the minimum, maximum, and average pre-scour barrel velocities and post-testing cross sectional scour depths at culvert stations 0, 4, 8, 12, and 16 for each test and the corresponding  $H_w/D$  ratio are presented in Table 4. Apart from general bed degradation, local abutment-type inlet scour was observed to occur for the 33 and 75% inlet contraction geometries. As scour occurred, the local velocities would slowly decrease until the bed material became stable and reached equilibrium.

**Table 4** Duration test scour results

Inlet test	Config. <sup>†</sup>	$H_w/D$	$V$ (m s <sup>-1</sup> )	Station				
				0	4	8	12	16
Scour depths (mm) [min/max/avg.]								
7-mm Gravel								
NP / 0%	0.50	0.77		0.0/-19.1/-8.9	0.0/-34.9/-19.1	0.0/-41.2/-15.9	0.0/-47.6/-26.0	-19.1/-47.6/-39.4
NP / 33%	0.50	0.77		0.0/-101.6/-52.1	-12.7/-31.8/-22.9	0.0/-47.6/-22.9	0.0/-47.6/-27.3	-25.4/-44.5/-36.8
NP / 75%	0.50	0.76		0.0/-108.0/-59.1	0.0/-31.8/-14.0	0.0/-34.9/-23.5	0.0/-44.5/-25.4	-25.4/-50.8/-40.0
P / 33%	0.50	0.59		-6.4/-76.2/-30.5	-3.2/-25.4/-15.2	0.0/-34.9/-20.0	-15.9/-50.8/-33.0	-15.9/-57.2/-40.0
P / 75%	0.50	0.71		-19.1/-146.1/-92.1	-6.4/-57.2/-33.0	-6.4/-57.2/-31.8	0.0/-57.2/-28.6	-60.3/-60.3/-60.3
16-mm Angular Gravel								
NP / 0%	1.00	1.26		-19.1/-41.3/-26.0	-25.4/-69.9/-47.6	-38.1/-82.6/-62.9	-50.8/-88.9/-69.9	-57.2/-101.6/-81.9
NP / 33%	1.00	1.09		6.4/-76.2/-26.7	-15.9/-63.5/-38.7	-25.4/-66.7/-49.5	-50.8/-82.6/-60.3	-57.2/-101.6/-77.5
NP / 75%	1.00	1.12		-6.4/-120.7/-73.7	-15.9/-57.2/-39.4	-41.3/-57.2/-52.1	-69.9/-76.2/-73.7	-76.2/-95.25/-87.0
P / 33%	1.00	0.97		-28.6/-155.6/-85.7	-57.2/-66.7/-62.2	-50.8/-101.6/-67.3	-63.5/-114.3/-86.4	-88.9/-111.1/-101.0
35-mm Cobbles								
NP / 0%	1.00	1.19		0.0/-25.4/-7.62	0.0/0.0/0.0	0.0/0.0/0.0	0.0/0.0/0.0	-12.7/-25.4/-19.1
NP / 0%	1.50	1.54		0.0/-50.8/-20.3	0.0/0.0/0.0	0.0/0.0/0.0	-6.4/-44.5/-27.0	-63.5/-108.0/-87.6
NP / 33%	1.00	1.01		0.0/0.0/0.0	0.0/0.0/0.0	0.0/0.0/0.0	0.0/0.0/0.0	0.0/0.0/0.0
NP / 33%	1.50	1.73		19.1/-82.6/-38.7	76.2/25.4/45.7	19.1/-50.8/-18.4	-57.2/-88.9/-67.3	-50.8/-88.9/-76.2
NP / 75%	1.00	1.00		0.0/0.0/0.0	0.0/0.0/0.0	0.0/0.0/0.0	0.0/0.0/0.0	0.0/0.0/0.0
NP / 75%	1.44	1.45		-28.6/-88.9/-62.9	19.1/0.0/7.0	12.7/-31.8/-7.6	-50.8/-101.6/-73.0	-79.4/-101.6/-91.4
P / 33%	1.00	1.03		0.0/0.0/0.0	0.0/0.0/0.0	0.0/0.0/0.0	0.0/0.0/0.0	0.0/0.0/0.0
P / 33%	1.50	1.51		-44.5/-146.1/-92.1	50.8/25.4/33.6	-19.1/-38.1/-26.7	-44.5/-76.2/-61.0	-82.6/-114.3/-96.5
P / 75%	1.00	1.03		0.0/0.0/0.0	0.0/0.0/0.0	0.0/0.0/0.0	0.0/0.0/0.0	0.0/0.0/0.0
P / 75%	1.49	1.61		-95.3/-139.7/-116.8	50.8/19.1/40.6	-50.8/-95.3/-69.9	-38.1/-76.2/-53.3	-82.6/-127.0/-99.1
37-mm Angular Rock								
NP / 0%	1.00	1.02		0.0/0.0/0.0	0.0/0.0/0.0	0.0/0.0/0.0	0.0/0.0/0.0	0.0/0.0/0.0
NP / 0%	1.50	1.53		0.0/-44.5/-21.6	0.0/0.0/0.0	0.0/-9.8/-19.1	-50.8/-111.1/-85.7	-63.5/-108.0/-87.0
NP / 33%	1.00	1.06		0.0/0.0/0.0	0.0/0.0/0.0	0.0/0.0/0.0	0.0/0.0/0.0	0.0/0.0/0.0
NP / 33%	1.50	1.55		-31.8/-101.6/-58.4	0.0/0.0/0.0	-12.7/-25.4/-18.4	-69.9/-101.6/-86.4	-69.9/-108.0/-87.6
NP / 75%	1.00	0.95		0.0/0.0/0.0	0.0/0.0/0.0	0.0/0.0/0.0	0.0/0.0/0.0	0.0/0.0/0.0
NP / 75%	1.50	1.54		-31.8/-101.6/-62.2	0.0/0.0/0.0	0.0/0.0/0.0	0.0/-57.2/-40.6	-85.7/-133.4/-108.6
P / 33%	1.00	0.99		0.0/0.0/0.0	0.0/0.0/0.0	0.0/0.0/0.0	0.0/0.0/0.0	0.0/0.0/0.0
P / 33%	1.50	1.43		0.0/-101.6/-59.7	25.4/0.0/10.2	0.0/0.0/0.0	12.7/-25.4/-11.4	0.0/-88.9/-43.2
P / 75%	1.00	0.95		0.0/0.0/0.0	0.0/0.0/0.0	0.0/0.0/0.0	0.0/0.0/0.0	0.0/0.0/0.0
P / 75%	1.50	1.31		-50.8/-101.6/-75.6	57.2/0.0/38.1	0.0/0.0/0.0	0.0/0.0/0.0	0.0/-114.3/-61.0

<sup>†</sup>NP = non-projecting, P = projecting, #% = inlet flow contraction

The 16-mm angular gravel substrate, as expected, was more resistant to scour than the 7-mm gravel substrate. Local scour holes, though smaller than those occurring during testing of the 7-mm gravel substrate, formed at the entrance of the culvert in response to the inlet flow contraction (33% and 75%). In addition, maximum depths of scour occurred at the exit region of the culvert and flow exiting the

culvert scoured a shallow channel in the tailbox. The bedform inside the culvert remained a flat plane during testing. An image of the streambed inside the culvert, looking upstream, after a  $H_w/D=1$  test, is presented in Fig. 5. Average scour depths at each station were observed to increase as the  $H_w/D$  ratio increased; the range of scour depths as a function of station are presented in Table 4.



**Fig. 5** Streambed scour looking upstream (A) 16-mm angular gravel, (B) 35-mm cobbles and (C) 37-mm angular rock

The 35-mm cobble substrate particles were not observed to slide and roll individually but rather in groups or clusters, which is attributed to the rounded shape of the substrate. Incipient motion was observed between  $1.25 < H_w/D < 1.5$ . No appreciable scour was observed for  $H_w/D < 1.4$ . A summary of the average barrel velocities and depths of scour at tested  $H_w/D$  ratios is presented in Table 4. Small localized scour holes at the entrance of the culvert began forming at  $H_w/D=1.0$ , generally of a depth equal to one particle diameter. The most considerable scour occurred inside the culvert barrel near the exit region of the culvert, and for the pressurized test scenarios, the streambed profile had a slight wave due to the water surface profile and deposition of material from the inlet. During scour, bed velocities measured at station 16 (exit) ranged from  $1.4$  to  $1.8 \text{ m s}^{-1}$ , with average culvert velocities (at the exit) ranging from  $1.5$  to  $2.1 \text{ m s}^{-1}$ .

As shown in Table 4, appreciable scour depths began to occur when the average culvert velocity exceeded  $1.1 \text{ m s}^{-1}$ . Corresponding average culvert velocities at the entrance of the culvert ranged from  $0.75$  to  $1.1 \text{ m s}^{-1}$ . These velocities were insufficient to cause appreciable scour except for two entrance conditions, 33% contraction projecting and 75% contraction projecting. These two entrance conditions resulted in flow vortices at locations A and E, producing measured bed velocities at each point ranging from  $1.1$  to  $1.3 \text{ m s}^{-1}$ . These results illustrate that local bed velocities may be larger than average flow velocities at locations of potential scour (such as entrance contractions or exiting jets) and should be taken into consideration. Potential scour areas are larger if pressurized flow conditions are likely to occur and it may be beneficial to use larger riprap materials at such locations and smaller material where acceptable.

The 37-mm angular rock substrate material was the most resistant to scour. Movement was observed to commence at slightly higher  $H_w/D$  ratios ( $1.3$  to  $1.5$ ) than the 35-mm cobble substrate. Though incipient motion conditions were similar for both substrates, the extent of scour that occurred was much less for the angular material. A comparison of the most pronounced scour that occurred during testing of the 37-mm angular rock and the 35-mm cobbles can be made utilizing Fig. 6. The results show that for the 37-mm angular substrate, 50% of the bed inside the culvert remained unchanged whereas 100% of the bed composed of the 35-mm cobbles changed. Scour depths and associated  $H_w/D$  ratios are presented in Table 4. The range of average depths of scour was from  $0$  to  $100\text{-mm}$ , with a maximum deposit depth at approximately  $45\text{-mm}$ . The location where scour was most severe was at station 16, at locations B, C, and D.

The bed velocities, which were measured when incipient motion occurred, ranged from  $1.1$  to  $1.3 \text{ m s}^{-1}$  at the entrance and  $1.4$  to  $1.8 \text{ m s}^{-1}$  at the exit. Generally, scour would become appreciable when average culvert velocities exceeded  $1.4 \text{ m s}^{-1}$ .

The 35-mm cobble substrate and 37-mm angular rock had similar  $d_{50}$  sizes, reached incipient motion under similar  $H_w/D$  ratios, attained similar local maximum depths of scour inside the barrel, and similar velocities were present during movement. However, two influential characteristics created a relatively large difference in the extent of scour inside the culvert, angularity and gradation. The scour results from these two substrates suggest that the most resilient bed material for bottomless arch culverts would not

only have particles of sufficient size to resist movement, but also be angular and well-graded. However, angular material may be less practical or more costly for streambed simulation as naturally occurring streambed material is rounded.

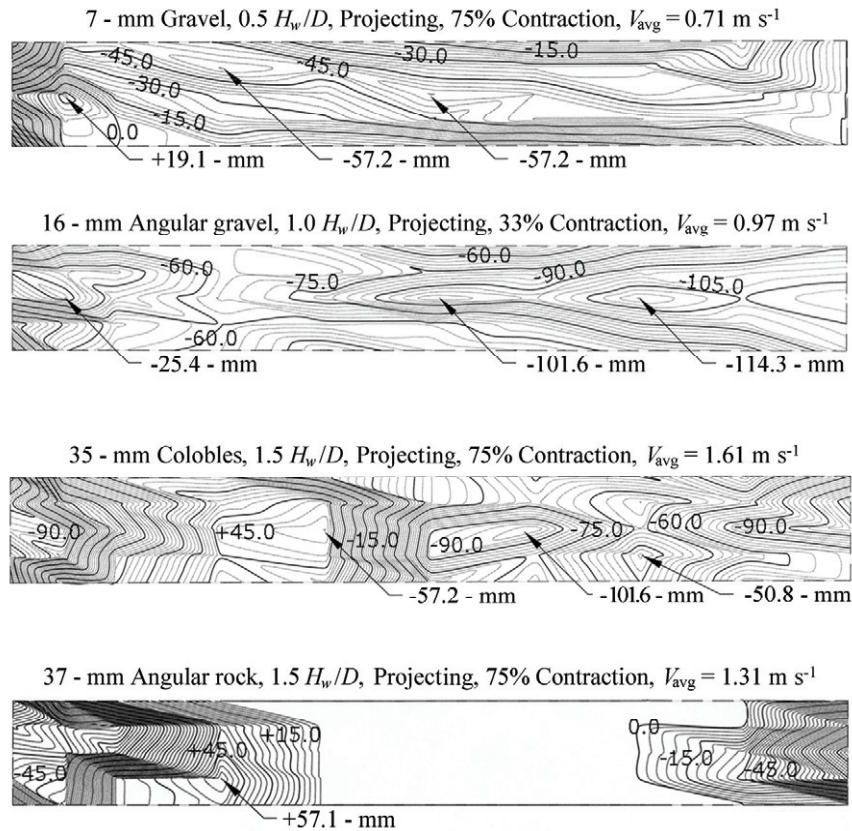


Fig. 6 Examples of bottomless arch culvert scour and deposition

#### 4 Riprap sizing methods

A means for scaling the experimental incipient motion results from this study to larger bottomless culvert applications would be beneficial, as the use of a 0.61-m diameter bottomless culverts for fish passage is less common. The State of California Department of Fish and Game, for example, specify a minimum culvert diameter for the streambed simulation design method of 1.83-m (6-ft). Two recently published FHWA methods, methods 1 and 2, and six well-established riprap sizing methods, Methods 3–8 (Table 1), were evaluated based on their ability to predict the minimum stone size required for a non-erodible substrate, using the experimentally determined average cross-section bed velocity at incipient motion as the independent variable. The objective was to evaluate the applicability of methods 1–8 as potential size-scaling relationships for bottomless culvert substrate stone sizing. The experimental results from the laboratory flume are an important component of this evaluation, as it provides a link between previous open-channel studies and the experimental results from the bottomless arch culvert. The results of the predicted and experimental stable  $d_s$  values are presented in terms of a factor of safety (ratio of  $d_s$  predicted over  $d_s$  actual). Factors of safety ( $SF$ ) for each substrate material tested in both the bottomless arch culvert and rectangular flume were calculated and plotted in Figs. 7 and 8.

As can be seen from comparing Figs. 7 and 8, the performance of some of the riprap stone sizing methods are application specific (i.e., bottomless culvert vs. the rectangular flume). In general,  $SF$  increased with increasing velocity for most methods in both the bottomless culvert and the rectangular flume.

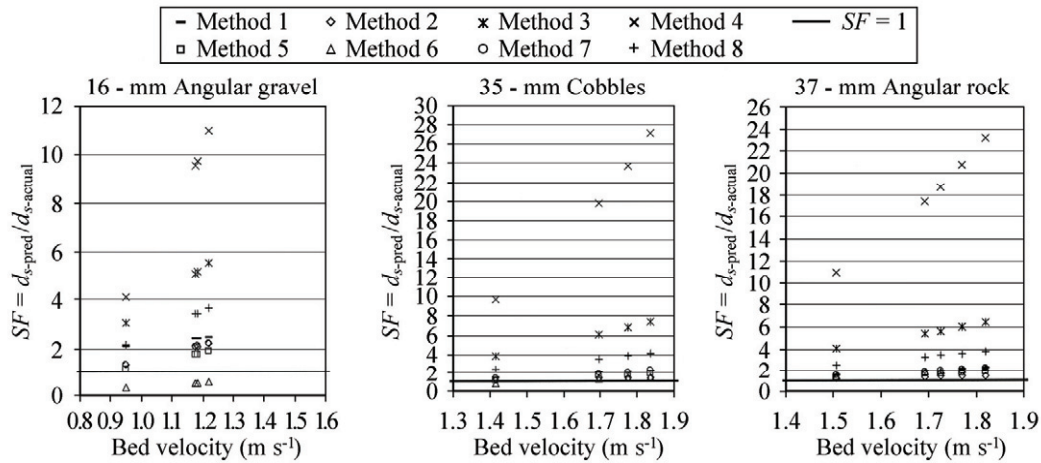


Fig. 7 Riprap safety factor comparison based on bottomless arch culvert incipient motion data

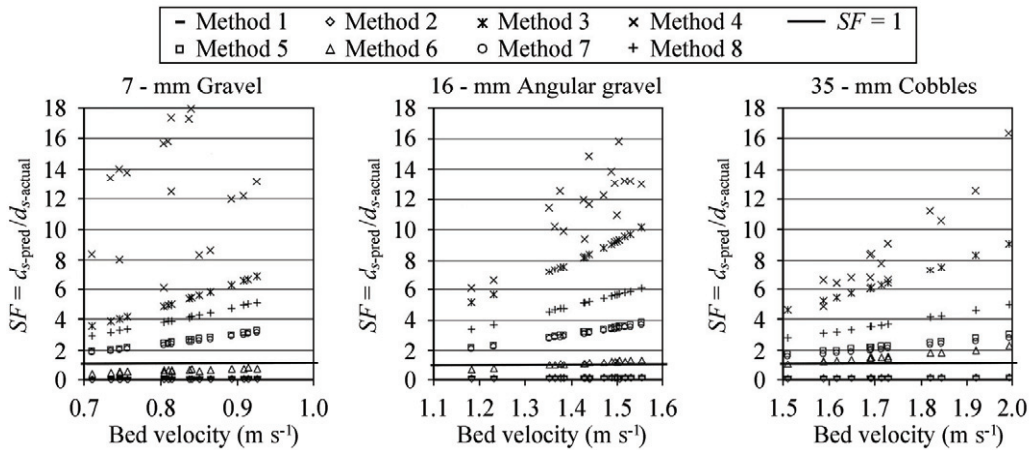


Fig. 8 Riprap safety factor comparison based on rectangular flume incipient motion data

Method 6 under-predicted stone sizes for the smaller substrate materials (7- and 16-mm), with  $SF$  ranging from 0.8 to 1 for the culvert and 0.5 to 1.5 for the flume data. For the larger substrate materials (35 and 37-mm),  $SF$  ranged from 1 to 2 for the culvert and flume data. It is important to note that in order to determine a  $d_{50}$  riprap stone size distribution using this method, flow velocity and flow depth data are required, along with condition-specific empirical coefficients, which must be determined or estimated.

Method 8 produced  $SF$  values ranging from approximately 3 to 6 in the laboratory flume and 2 to 4 for the 35-mm cobbles and the 37-mm angular rock. Method 3 produced  $SF$  values ranging from approximately 4 to 10 in the laboratory flume and approximately 4 to 6 in the 35-mm cobbles and the 37-mm angular rock substrate materials in the bottomless culvert. The large  $SF$  values suggest that this method may be over conservative, which may be attributed to its development for a 100-year flow event.

Method 4 was the most conservative method ( $SF$  often exceeding 10) and produced the most scatter, with the stone size increasing sharply with increasing velocity. This method may be too conservative for bottomless culvert applications. In addition, Halvorson and Laumann (1996) also found HEC-11 overly conservative. Blodgett and McConaughy (1986) indicate in their study that the results of HEC-11 were unsatisfactory or the application was not appropriate due to application limitations. Method 5 predicted  $SF$  values ranging from approximately 2 to 4 in the laboratory flume, but only 1 to 2 in the bottomless culvert. Method 7 produced very similar results to the CAL B&SP stone prediction method, which agrees with published literature cited previously.

The results methods 1 and 2 were very similar and predicted factors of safety comparable to methods 5 and 7 in the bottomless arch culvert. Methods 1 and 2, however, under predicted stone sizes in the

laboratory flume and therefore appear to be specific to culvert applications. When selecting a stone sizing method for an application (e.g., bottomless culvert, trapezoidal channel, etc.) it is important to have a general sense of performance as some appear to be best suited for culverts and others for trapezoidal cross-sections.

Although all 8 methods are to some degree empirical equations, there are notable performance differences that can be attributed to the level of empiricism. Methods 5, 6 and 7 are the least empirical and performed favorably in both the rectangular flume and the bottomless arch culvert; methods 5 and 7 are identical except for the value of a singular constant. Method 1 and 2 also performed favorably in the bottomless arch culvert, however they are empirical equations developed for culvert application. Methods 3, 4, and 8 have the highest level of empiricism (note the similarity of methods 3 and 8). These methods were the most conservative when evaluated against the experimental results of this study.

When implementing a riprap design method, it is important to refer to the original publication for any additional guidelines, limitations, or additional information. Site-specific information should also be obtained, where possible, to identify specific hydraulic conditions the riprap will experience. The accuracy of each riprap design method hinges on the correct estimation of input parameters. This investigation found methods 1, 2, 5, 6, and 7 to require additional safety factors (inherit  $SF$  of 1 to 2 for the 35- and 37-mm gravels) when applied to bottomless arch culverts. These methods are recommended as designers are able to select their own factors of safety for larger installations.

## 5 Conclusion

By creating favorable hydraulic conditions for aquatic life and simulating the natural streambed, bottomless culverts can be acceptable ecological passageways. Bottomless culverts should be designed not only for base flow conditions, but also for high flow events. This study presents experimental results of the scour behavior of a bottomless culvert under pressurized and non-pressurized conditions to aid in bottomless culvert design. Riprap is a viable option for protecting streambeds through bottomless culverts during high flow events. Relative conservativeness or factors of safety of eight available stone sizing were evaluated to aid designers in selecting a stone sizing method.

Four substrate materials were evaluated in a 0.61-m wide bottomless arch culvert under pressurized and non-pressurized flow conditions with a variety of entrance configurations. Scour occurred along the entire length of the culvert, with the most severe scour occurring at the entrance and exit regions. Flow contraction caused local pier-type scour holes at the culvert entrance. In addition, bed degradation occurred at the culvert entrance during pressurized flows. There was no controlled tailwater, therefore the highest velocities and maximum scour depths were recorded at the culvert exit. Angularity and gradation decreased the extent of scour inside the culvert barrel, compared to rounded cobbles that may be more common for streambed simulation.

Incipient motion of the four tested substrates was also investigated and compared to the predicted results of eight riprap stone sizing methods (presented in Figs. 7 and 8); these methods were selected in an effort to scale the experimental results of this study to larger bottomless culvert sizes. Furthermore, incipient motion investigations also included a rectangular flume to explore the influences of cross-sectional geometry on the riprap stone sizing method results.

Methods 1 and 2 produced safety factors ranging from 1 to 3 in the culvert and 0 to 0.3 in the rectangular flume. Method 3 was more conservative, producing  $SF$  values ranging from 3 to 8 in the culvert and 3 to 10 in the flume. Method 4 produced the most conservative and scattered  $SF$  values in the bottomless culvert, and slightly less conservative values in the rectangular flume, at 4 to 28 and 6 to 18, respectively. Methods 5, 7, and 8 produced similar  $SF$  values ranging from 1 to 4 in the culvert and 2 to 6 in the flume. Finally, method 6 produced  $SF$  values of 0.5 to 2 in the culvert and rectangular flume.

The high level of conservatism for method 4 may be attributed to the application of a 1-dimensional modeling tool to a 2- and 3-dimensional flow conditions. Also, methods 1 and 2 were less conservative in the rectangular flume as each was developed for culverts. Methods 1, 2, and 5–7 all produced factors of safety approximately between 1 and 2 in the larger tested substrate materials in the bottomless culvert, with factors of safety slightly increasing with increasing bed velocities. These methods appear to be the best for designers as they would be able to choose their own factors of safety in larger installations. Methods 3 and 7 appear to already contain factors of safety in the larger materials of 4 to 8 and 2 to 4, respectively.

Additional research in this area should include: testing larger bottomless culvert diameters; determining the influence of sidewall roughness, such as corrugations, on bottomless culverts scour; evaluate larger stone sizes; and streambed materials with fine material present (non-armored beds). This additional research would help to identify the most appropriate scaling methods as well as limitations for determining stable bottomless culvert streambed material sizes for field applications.

### **Acknowledgements**

Funding for this study was provided by the Alaskan Department of Transportation and Public Facilities and the State of Utah (Utah Water Research Laboratory).

### **References**

- Abida H. and Townsend R. D. 1991, Local scour downstream of box-culvert outlets. *Journal of Irrigation and Drainage*, ASCE, Vol. 117, No. 6, pp. 25–40.
- Abt S. R. 1980, Scour at culvert outlets in cohesive bed material. Ph.D. Dissertation, Colorado State University, Fort Collins, Colo.
- Abt S. R., Kloberdanz R. L., and Mendoza C. 1984, Unified culvert scour determination. *Journal of Hydraulic Engineering*, Vol. 110, No. 10, pp. 1475–1479.
- Abt S. R., Ruff J. F., and Doehring F. K. 1985, Culvert slope effects on outlet scour. *Journal of Hydraulic Engineering*, ASCE, Vol. 111, No. 10, pp. 1363–1367.
- Abt S. R. and Thompson P. L. 1996, Scour at culvert outlets: Considerations present and future. *Streambed Stability and Scour at Highway Bridges*, pp. 3927–3931.
- Bates K., Barnard B., Heiner B., Klavas J. P., and Powers P. D. (WDF&D). 2003, Fish passage design at road culverts. Washington Department of Fish and Wildlife, Olympia.
- Blodgett J. C. and McConaughy C. E. 1986, Rock riprap design for protection of stream channels near highway structures: Volume 2 – Evaluation of riprap design procedures. Water Resources Investigations Report 86-4128, Sacramento, Calif.
- Bohan J. P. 1970, Erosion and riprap requirements at culvert and storm-drain outlets, Research Report H-70-2, U.S. Army Engineer Waterways Experiment Station, Vicksburg, Miss.
- California Department of Fish and Game (CDFG). 2002, Culvert criteria for fish passage. Fisheries Branch Publications, <[http://www.dfg.ca.gov/nafwb/pubs/2002/culvert\\_criteria.pdf](http://www.dfg.ca.gov/nafwb/pubs/2002/culvert_criteria.pdf)> (July 9, 2007).
- California Department of Public Works, Division of Highways (Cal B&SP). 1970, Bank and shore protection in California highway practice. Sacramento, Calif.
- Chien N. Wan Z., and McNown J. S. (Translator). 1998, *Mechanics of Sediment Transport*. American Society of Civil Engineers, Reston, Va.
- Crookston B. M. 2008, A laboratory study of streambed stability in bottomless culverts. M.S. Thesis, Utah State University, Logan, Utah.
- Crookston B. M. and Tullis B. 2011, Incipient motion of gravels in a bottomless arch culvert. *International Journal of Sediment Research*, Vol. 26, No. 1, 2011, pp. 15–26.
- Federal Highway Administration (FHWA). 2003, Bottomless culvert scour study: Phase 1 laboratory report. FHWA-RD-02-078, Federal Highway Administration, D.C.
- Federal Highway Administration (FHWA). 2007, Bottomless culvert scour study: Phase 2 laboratory report. FHWA-HRT-07-026. Federal Highway Administration, D.C.
- Federal Highway Administration (FHWA). 1989, Use of riprap for bank protection. Hydraulic Engineering Circular #11 (HEC 11). FHWA-IP-89-016, Federal Highway Administration, D.C.
- Halvorson, D. V. and Laumann F. J. 1996, Scour protection in bottomless culverts. *North American Water and Environment Congress & Destructive Water*, pp. 3932–3941.
- Maynard S. T. 1979, Practical riprap design, U.S. Army Waterways Experiment Station, Misc. Paper H-78-7, Vicksburg, Miss.
- Maynard S. T. 1987, Stable riprap size for open channel flows. Ph.D. Dissertation, Colorado State University, Fort Collins, Colo.
- Mendoza C., Abt S. R., and Ruff J. F. 1983, Headwall influence on scour at culvert outlets. *Journal of Hydraulic Engineering*, Vol. 109, No. 7, pp. 1056–1060.
- Shafai-Bajestan M. and Albertson M. L. 1993, Riprap criteria below pipe outlet. *Journal of Hydraulic Engineering*, Vol. 119, No. 2, pp. 181–200.
- U.S. Army Corps of Engineers (USACE). 1994, Hydraulic design of flood control channels: Engineering manual. EM 1110-2-1601. D.C.
- U.S. Bureau of Reclamation (USBR). 1962, Studies of tractive forces of cohesive soils in earth canals: Division of engineering laboratories. Hydraulics Division, Reports of Engineering Practice No. 504, New York.

- Vanoni V. A. 2004, Sedimentation engineering, ASCE manual No. 54. American Society of Civil Engineers, Sedimentation Committee of Hydraulics Division, New York.
- Yalin M. S. 1972, Mechanics of sediment transport. Pergamon Press, Oxford, New York, pp. 74–110.
- Yang C. T. and Simões J. M. 2005, Wash load and bed-material load transport in the yellow river. Journal of Hydraulic Engineering, Vol. 131, No. 5, pp. 413–418.

#### Notation

- $A$  = observed area for incipient motion;
- $C$  = safety factor with published values specific to channel geometry and severity of attack by current;
- $C_T$  = thickness coefficient;
- $C_V$  = vertical velocity distribution coefficient;
- $d_s$  = a representative particle size diameter where  $s$  represents the percent of material in a sample that is smaller than the representative particle size (i.e.,  $s=30, 40, 50 \dots$ ).
- $D$  = distance between the pre-scour culvert streambed invert and the culvert crown;
- $\varepsilon$  = criterion for incipient motion proposed by Yalin (1972);
- $\gamma$  = specific weight of water;
- $\gamma_s$  = average specific weight of substrate material;
- $g$  = acceleration constant of gravity;
- $H_w$  = total upstream headwater measures relative to the inlet pre-scour culvert invert;
- $N$  = number of particles in motion for a given area;
- $\rho$  = mass density of fluid;
- $SF$  = safety factor, ratio of  $d_{s\_predicted}$  to  $d_{s\_actual}$ ;
- $SG$  = specific gravity of riprap material;
- $t$  = time interval for incipient motion observation;
- $V_{ent}$  = average velocity at the culvert entrance;
- $V_{eff}$  = effective local bed velocity;
- $V$  = average cross-sectional culvert velocity at location of interest;
- $Y$  = local flow depth;
- $Y_{ent}$  = depth of flow at the culvert entrance.